

Electronic structure of monoclinic $\text{TeMo}_5\text{O}_{16}$: Prediction of semiconducting behavior

Josep M. Oliva, Pablo Ordejón, and Enric Canadell

Institut de Ciència de Materials de Barcelona (CSIC), Campus de la Universitat Autònoma de Barcelona, Bellaterra, E-08193 Barcelona, Spain

(Received 6 June 2000)

The electronic structure of monoclinic $\text{TeMo}_5\text{O}_{16}$, a molybdenum oxide recently reported and expected to be a new low-dimensional metal, has been studied by means of first principles density functional calculations. The study predicts that monoclinic $\text{TeMo}_5\text{O}_{16}$ should not be metallic (as previously suggested on the basis of a bond length–bond valence analysis) but semiconducting. The structural origin of the energy gap is analyzed in detail.

I. INTRODUCTION

Some molybdenum and tungsten oxides and bronzes are low-dimensional metals and exhibit very interesting physical properties.^{1–8} Either real or “hidden” nesting in their Fermi surface^{8,9} leads to electronic instabilities that are at the origin of their anomalous low-temperature physical behavior. Despite intensive work on these low-dimensional materials many problems still remain unanswered. For instance, the detailed microscopic mechanism for the successive structural modulations in monophosphate tungsten bronzes, the origin of the low-temperature resistivity upturn in the lithium purple bronze, and the possibility of a Luttinger-type behavior for some of these materials are questions of debate. It is clear that our understanding of the physics of these materials is still fragmentary. Under such circumstances it is very important to find new materials of this class, which can be the subject of detailed structural and physical measurements. This should lead to some progress in our understanding of their physics and that of the low-dimensional metals in general.

Recently, Vallar and Goreaud¹⁰ have reported the crystal structure of monoclinic $\text{TeMo}_5\text{O}_{16}$ (see Fig. 1), which contains four formula units in the unit cell. The simplest way to describe the three-dimensional Mo—O network of this phase is by considering it as resulting from the condensation of a series of perovskite type double octahedral Mo_8O_{28} slabs perpendicular to the a direction [thus involving the Mo(2), Mo(3), Mo(4), and Mo(5) octahedra; see Fig. 1]. These slabs are brought together into the $\text{Mo}_{10}\text{O}_{32}$ three-dimensional network of $\text{TeMo}_5\text{O}_{16}$ by sharing the outer oxygen atoms with the basal oxygens of a series of Mo(1)O₆ octahedra. It is in the holes between the different Mo(1)O₆ octahedra that the tellurium atoms reside. These Te atoms are quite shifted from the center of the cavities and make three Te—O bonds in such a way that the Te atoms reside at one of the vertices of an approximate TeO₃ trigonal pyramid (one of the three Te—O bonds can not be seen in Fig. 1 because it involves an oxygen atom which lies just on top or below the Te atom). Consequently, the Te atoms bear an electron lone pair and must be considered as Te(IV).

Using the formal oxidation states of O²⁻ and Te⁴⁺ only two electrons per formula unit (i.e., eight electrons per unit cell) are left to fill the Mo d -block bands. In order to have some idea of how delocalized these electrons are, Vallar and Goreaud¹⁰ carried out a bond length–bond valence analysis¹¹

of the crystal structure. This type of analysis has been very useful in understanding the dimensionality of several molybdenum oxides and bronzes.¹² These authors found that the effective charge of Mo(1) was practically +6 whereas those of the Mo(2) to Mo(5) atoms were all around +5.5. From this they concluded that the Mo d electrons should be delocalized on the double octahedral slabs formed by the Mo(2), Mo(3), Mo(4), and Mo(5) octahedra and that these slabs should be isolated from each other by the Mo(1) octahedra. $\text{TeMo}_5\text{O}_{16}$ was thus predicted to be a two-dimensional conductor very similar to the potassium purple bronze $\text{KMo}_6\text{O}_{17}$ or the Magnéli γ - and η - Mo_4O_{11} phases, which indeed exhibit very interesting electronic instabilities. Thus, $\text{TeMo}_5\text{O}_{16}$ could be a very interesting new material to study provided that it really exhibits a metallic behavior. Since no resistivity measurements were reported by Vallar and Goreaud¹⁰ we decided to consider this question by carrying out first principles density functional calculations.

II. COMPUTATIONAL DETAILS

The calculations were done using a numerical atomic orbitals density functional theory^{13,14} (DFT) approach, which has been recently developed and designed for efficient calculations in large and low symmetry systems and implemented in the SIESTA code.^{15–19} We have used the generalized gradient approximation to DFT, and in particular the functional of Perdew, Burke, and Ernzerhof.²⁰ Only the valence electrons are considered in the calculation, with the core being replaced by norm-conserving scalar relativistic pseudopotentials²¹ factorized in the Kleinman-Bylander form.²² For Mo and Te, we include nonlinear partial-core corrections²³ to describe the exchange and correlation in the core region since for these elements the core and the valence charges overlap significantly. The pseudopotentials were generated using the following configurations: $2s^22p^4$ for O, $5s^14d^5$ for Mo, and $5s^25p^4$ for Te. The cutoff radii were 1.14 a.u. for all the components in oxygen, 2.5, 3.1, 2.1, and 2.2 a.u. for the s , p , d , and f components in molybdenum, respectively, and 2.0, 2.0, and 3.0 a.u. for the s , p , and d components of tellurium, respectively.

The valence one-particle problem was solved using a linear combination of numerical (pseudo) atomic orbitals (PAO's) with finite range r_c .²⁴ The numerical values of the orbitals are stored in tables as a function of the distance from the nucleus, for a mesh of about 500 points. The details of

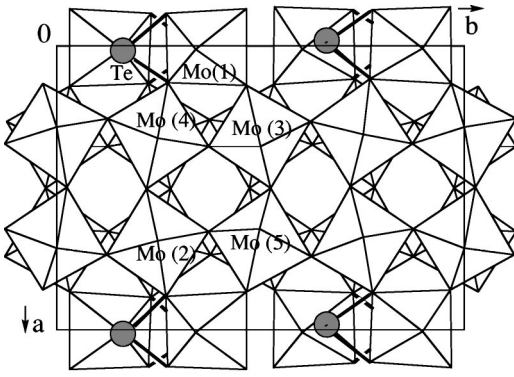


FIG. 1. Projection along the c axis of the crystal structure of monoclinic $\text{TeMo}_5\text{O}_{16}$.

the basis generation (including multiple- ζ and polarization functions) can be found in Ref. 18, and here we only give a brief overview. The shape of the confined orbitals is obtained by solving the atomic problem with the given pseudopotential, and imposing that the wave function vanishes at the chosen confinement radius r_c ,^{24,18} whose value is different for each orbital on each atom. The confinement radii of the different orbitals is determined by a single parameter, the *energy shift*, which is the energy increase of the atomic eigenstate due to the confinement. Specifying this parameter defines all radii in a well balanced way, and allows the systematic convergence of physical quantities to the required precision.¹⁸ To generate confined multiple- ζ bases, we use¹⁸ an implementation of the split-valence scheme of quantum chemistry: the numerical PAO's are split in two (or more): the first reproduces the tail of the original PAO beyond some radius R_m , and continues smoothly towards the origin; the second one is the difference between the original orbital and the one reproducing the tail. In this way, multiple splits can be performed successively to generate multiple- ζ bases. The choice of the matching radius R_m for all the orbitals in all the atoms is done, again, by means of a single parameter: the *split-norm*, which determines the norm of the original orbital which is kept in the tail beyond R_m . Polarization orbitals are obtained by computing the response of the occupied atomic wave functions to the presence of a small external electric field.¹⁸ In this work, we have used a split-valence double- ζ basis set, as obtained with an energy shift of 500 meV and a split-norm of 15%. Some tests were also done using the same basis set, but including polarization orbitals in all the atoms, as we will explain below.

The integrals of the self-consistent terms of the Kohn-Sham Hamiltonian are obtained with the help of a regular real space grid in which the electron density is projected. The Hartree potential is calculated by means of fast Fourier transforms in that grid. The grid spacing is determined by the maximum kinetic energy of the plane waves that can be represented in that grid. In the present work, we used a cutoff of 100 Ry, which yields to a spacing between grid points of around 0.16 Å. The Brillouin zone (BZ) was sampled using a grid of 64 k -points. We have checked that the results are well converged with respect to the real space grid, the BZ sampling and the range of the atomic orbitals.

The method sketched above has already been applied to a large number of very different systems,¹⁹ among others tran-

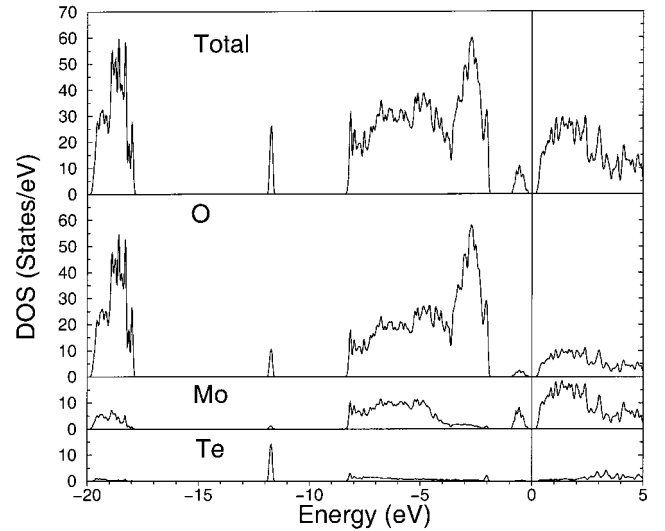


FIG. 2. Total and projected density of states of monoclinic $\text{TeMo}_5\text{O}_{16}$ projected onto the Mo, O, and Te sites.

sition and noble metals systems,^{25–28} semiconductors (including surfaces and liquids),^{29–32} carbon nanostructures,^{33–36} and oxides (including ferroelectric perovskites and blue bronzes).^{37,38}

The calculations presented here were carried out using the experimental crystalline structure (atomic positions and lattice parameters), obtained by Vallar and Goreaud (see Table 1 of Ref. 10).

III. RESULTS AND DISCUSSION

A. Electronic structure

The calculated density of states and band structure near the Fermi level are reported in Figs. 2 and 3, respectively. The density of states diagram of Fig. 2 (which was obtained by broadening the eigenvalue spectrum calculated with the 64 k -point sampling with a Gaussian of width 0.05 eV) exhibits a strong mixing between the Mo and O states as well as between the Te and O ones. This clearly shows the strong covalent character of the binding in these phases. Of special

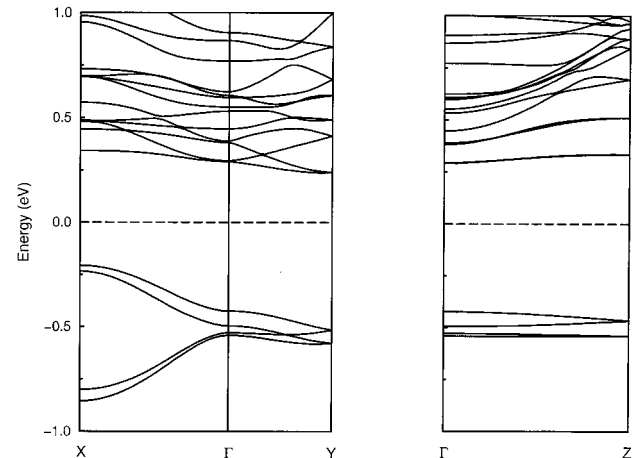


FIG. 3. Band structure for monoclinic $\text{TeMo}_5\text{O}_{16}$. $\Gamma = (0, 0, 0)$, $X = (1/2, 0, 0)$, $Y = (0, 1/2, 0)$, and $Z = (0, 0, 1/2)$ in units of the monoclinic reciprocal lattice vectors.

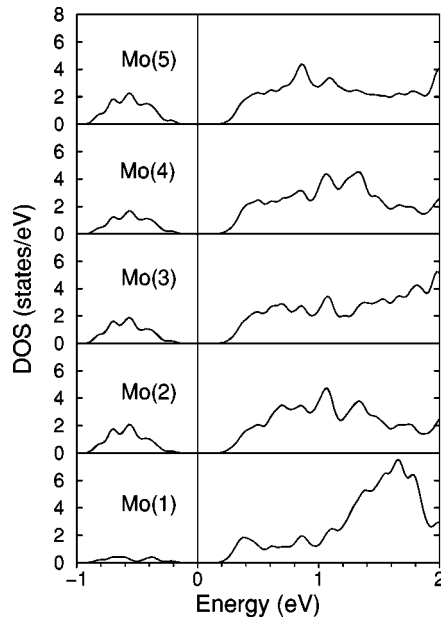


FIG. 4. Projected density of states associated with the five different types of Mo sites (see Fig. 1 for labeling).

interest for the problem at hand is the fact that two different energy gaps appear near the Fermi level. The one around -1.5 eV separates the mainly Mo contributions above the cap from the mainly O contribution below the gap (we remark again that there is a significant mixing, and therefore the separation is not clear cut; we also note that the density of states shown in Fig. 2 reflects the contribution of the 16 O atoms and the 5 Mo atoms in the unit cell, so the apparently large DOS for O above the gap is partly due to the larger number of atoms compared to Mo). When all the states up to the lowest gap are filled there remain two electrons per formula unit to fill the Mo states. The second gap, which appears in the lower part of the Mo states, is associated with four well-separated energy bands (see Fig. 2) and thus the eight electrons per unit cell left to fill the Mo states will completely fill the levels below this second gap. Consequently, monoclinic $\text{TeMo}_5\text{O}_{16}$ is predicted to be a regular semiconductor with an indirect gap of around 0.50 eV.²⁵ Inclusion of polarization functions in the basis set ($5d$ for Te, $5p$ for Mo, and $3d$ for O) only slightly decrease the gap to 0.47 eV so that the existence of an indirect band gap at the Fermi level does not depend on the details of the calculation.

B. Origin of the energy gap

The opening of the gap at the Fermi level does not only have important consequences for the physical behavior of the material, but it is surprising in view of the general success of the bond length–bond valence correlations in rationalizing the transport properties of low-dimensional molybdenum oxides and bronzes. Thus, we now try to understand the most important feature of the band structure of Fig. 3, i.e., the opening of a band gap for precisely two electrons per formula unit filling the Mo-based bands of this system.

We just need to consider the lowest-lying t_{2g} bands and how the distortions of the different MoO_6 octahedra control their topology. The analysis is quite simple because the t_{2g} levels of an MoO_6 octahedron have antibonding combina-

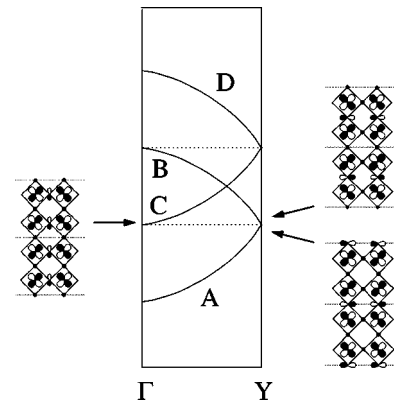


FIG. 5. Schematic illustration of the Mo xy -based bands of an ideal Mo_4O_{18} octahedral chain (all O—Mo—O angles of 90° and identical in-plane Mo—O bond lengths) along b with a strong O—Mo \cdots O bond length difference perpendicular to the chain direction. For simplicity the p orbitals of the unshared oxygen atoms are not shown in the schematic representation of the crystal orbitals, and dots are used to indicate the absence of the p orbital contribution from the shared oxygen atoms.

tions between the Mo d orbitals and the O p orbitals. Hence, a shortening of an Mo—O bond length raises the energy of the t_{2g} orbital, which has an antibonding combination between the Mo and O orbitals along that bond. Because of the shape of the t_{2g} orbitals, the shortening of a Mo—O bond raises two of the three t_{2g} orbitals and leaves the other, which is of δ type with respect to the shortened Mo—O bond, unaltered.⁸ An important feature of the structure of monoclinic $\text{TeMo}_5\text{O}_{16}$ is that all octahedra exhibit a strong O—Mo \cdots O bond length difference along the c direction [1.68 vs 2.12 Å for Mo(1), 1.70 vs 2.38 Å for Mo(2), 1.70 vs 2.45 Å for Mo(3), 1.69 vs 2.39 Å for Mo(4), and 1.68 vs 2.42 Å for Mo(5)], and in all cases the short bond is considerably shorter than a standard octahedral Mo—O bond length (1.95 Å). Consequently, only one t_{2g} level of any MoO_6 octahedra (i.e., the orbital approximately contained in the ab plane to which we will refer in the following as the xy orbital) can contribute to the lower-lying t_{2g} -block bands.

The band dispersion will thus arise as a consequence of the antibonding interactions between the Mo xy orbitals and the p orbitals of O. Since the Mo xy orbitals are of δ type with respect to the c direction, the p orbitals of the O atoms between the Mo—O planes practically cannot mix with them and the lowest-lying t_{2g} -type bands should be practically dispersionless in that direction. Thus, from the viewpoint of the bands in which we are interested, monoclinic $\text{TeMo}_5\text{O}_{16}$ could be considered to be a two-dimensional system. However, the orbital interactions leading to the band dispersion would not run along the bc planes, as implied by the suggestion of Vallard and Goreaud,¹⁰ but along the ab planes. Thus, what we need to consider is the interaction between the Mo xy orbitals through the O x and y orbitals.

The simplest way to approach the problem is by considering the octahedral planes perpendicular to the c direction as resulting from the condensation of the Mo_4O_{18} chains [i.e., those formed by the Mo(2), Mo(3), Mo(4), and Mo(5) octahedra] and Mo(1) O_6 octahedra. Model extended Hückel calculations for the five different MoO_6 octahedra in the structure show that the xy orbital of the Mo(1) octahedra is

higher-lying than those of the remaining four octahedra. The five octahedra have two short and two long Mo—O bonds in the *ab* planes but the two short ones of the Mo(1) octahedra are considerably shorter (1.80 Å) than those of the other octahedra (between 1.85 and 1.89 Å). Since the short bonds are those that control the raising of the *xy* orbital, the one of Mo(1) lies higher in energy and consequently, the low-lying *xy* orbitals of the Mo(2)–Mo(5) octahedra are those which are going to be the main components of the lowest-lying t_{2g} -block bands of monoclinic $\text{TeMo}_5\text{O}_{16}$. This qualitative analysis is substantiated by the projected densities of states of Fig. 4: the bands between 0 and -1 eV are mainly built from the Mo(2)–Mo(5) orbitals with only a substantially smaller contribution of those of Mo(1).

The nature of the *xy* bands of an ideal octahedral Mo_4O_{18} chain with a strong O—Mo \cdots O bond length difference perpendicular to the chain direction (see Fig. 5), and how different distortions influence these bands, has been analyzed in detail by Canadell and Whangbo and co-workers^{8,40,41} in order to rationalize the transport properties of related molybdenum oxides and bronzes. Important for the present work is the relative position of bands *A* and *B* at *Y* and band *C* at Γ . The fact that in the real chain the Mo—O bond lengths along the chain direction are different must open a gap between bands *A* and *B* at *Y*. Thus, if band *A* at *Y* remains lower in energy than band *C* at Γ , one filled band per formula unit of monoclinic $\text{TeMo}_5\text{O}_{16}$ should be left alone at the bottom of the Mo-based bands of the solid. Since there are two electrons per formula unit to fill the t_{2g} -type bands, this would explain the semiconducting character of the material provided that the coupling through the Mo(1) *xy* orbitals between bands *A* of adjacent Mo_4O_{18} chains is not large enough to close the gap along the a^* direction. However, this coupling cannot be very strong because, as noted above, the mixing of the Mo(1) *xy* orbitals into these bands is relatively small.

The main orbital components of bands *A* and *B* at *Y* and band *C* at Γ are schematically shown in Fig. 5. For simplicity the *p* orbitals of the unshared oxygen atoms are not shown in the figure, and dots are used to indicate the absence of the *p* orbital contribution from the shared oxygen atoms. From these orbital diagrams it is easy to understand the degeneracy of the three band levels in the ideal chain: they have the same number of antibonding oxygen *p* orbital contributions (i.e., two per unit cell). Bands *A* and *B* are no longer degenerate in the real chain because there is an O \cdots Mo—O—Mo \cdots O type alternation along the chain direction. The real chain also has an O \cdots Mo—O—Mo \cdots O type alternation in the direction perpendicular to the chain direction. Since the short Mo—O distances perpendicular to the chain axis are shorter than the long Mo \cdots O distances along the chain direction, band *C* at Γ is higher in energy than band *A* at *Y*. Thus, in the real chain, band *A* should stay below all other bands. As shown in Fig. 3, the four well-separated low-lying bands of this type (remember that there are four formula units per unit cell) are flat along the chain direction and show some dispersion along a^* . The first observation is the result of both the bond length alternation along the chain direction and the octahedral rotations (see Fig. 1) that decrease the π -type overlap between the Mo *xy* and O *x* orbitals. The dispersion along a^* comes out from the mixing of

the higher lying Mo(1) *xy* orbitals into band *A*, establishing a bridge between the different chains.

A Mulliken population analysis of the wave function shows that the total electronic charge associated with the different Mo atoms is very similar. Since Mo(2)–Mo(5) are the main contributors to the four low-lying filled t_{2g} bands, this means that Mo(1) has a larger contribution to the more heavily oxygen-based filled bands. This is expected because, as noted above, the Mo(1)O₆ octahedra have two considerably shorter Mo—O bonds and thus the contribution of Mo(1) to these bands, which are those describing the Mo—O bonding, must be somewhat larger. The similarity in the Mo charges is in contrast with the large difference ($0.5e$) reported by Vallar and Goreaud¹⁰ from the empirical bond length–bond valence analysis. However, when the Mulliken population analysis was carried out for just the four lower-lying Mo-based bands it was found that the contribution of the Mo(1) orbitals ($0.09e$) was only approximately one fourth of those of any of the other Mo atoms [$(0.3 - 0.4)e$], in agreement with our analysis above. This is at least partially in agreement with the results of Vallar and Goreaud.¹⁰ Yet, the bond length–bond valence correlations, by just taking into account the bond lengths around the transition metal atom (i.e., neglecting the directionality of bonding, the relative distribution of short and long Mo—O bonds, etc), cannot describe accurately enough the relationship between the crystal and electronic structure of complex materials.

IV. CONCLUSIONS

Our work predicts that monoclinic $\text{TeMo}_5\text{O}_{16}$ should be an indirect gap semiconductor and not a two-dimensional metal as it could have been expected from previous work. Our detailed analysis makes clear the structural origin of this fact. Three features of the crystal structure are essential: (i) the strong O—Mo \cdots O bond length difference along the *c* direction. (ii) the stronger distortion in the Mo(1)O₆ octahedra, imposed by the tellurium atoms that make bonds with two of the basal oxygen atoms, leading to high-lying Mo(1) *xy* orbitals, and (iii) the relative values of the short Mo—O distances perpendicular to the chain axis with respect to the long Mo \cdots O distances along the chain direction. It is interesting to note that WO₆ octahedra with very low *d*-electron counts are usually considerably less distorted than the corresponding MoO₆ ones. Thus the tungsten analog of monoclinic $\text{TeMo}_5\text{O}_{16}$ could well be a more interesting material. In fact, tungsten analogs of related materials are known⁴² and therefore work along this line would be worthwhile.

ACKNOWLEDGMENTS

This work was supported by the DGES-Spain Project PB96-0859 and by Generalitat de Catalunya (1999 SGR 207). P.O. acknowledges support from Fundaci3n Ram3n Areces (Spain). J.M.O. acknowledges the Ministerio de Educaci3n y Cultura (Spain) for a contract of the Programa de Incorporaci3n de Doctores y Tecn3logos. The computations described in this work were carried out using the resources of CESCA and CEPBA coordinated by C⁴.

- ¹ *Low-Dimensional Electronic Properties of Molybdenum Bronzes and Oxides*, edited by C. Schlenker (Kluwer, Dordrecht, 1989).
- ² *Physics and Chemistry of Low-Dimensional Inorganic Conductors*, edited by C. Schlenker, J. Dumas, M. Greenblatt, and S. van Smaalen, Vol. 354 of NATO ASI Series B, Physics (Plenum, New York, 1996).
- ³ M. Greenblatt, *Int. J. Mod. Phys. B* **7**, 3937 (1993).
- ⁴ P. Foury and J. P. Pouget, *Int. J. Mod. Phys. B* **7**, 3973 (1993).
- ⁵ E. Canadell and M.-H. Whangbo, *Int. J. Mod. Phys. B* **7**, 4005 (1993).
- ⁶ J. Dumas and C. Schlenker, *Int. J. Mod. Phys. B* **7**, 4045 (1993).
- ⁷ M. Greenblatt, *Chem. Rev.* **88**, 31 (1988).
- ⁸ E. Canadell and M.-H. Whangbo, *Chem. Rev.* **91**, 965 (1991).
- ⁹ M.-H. Whangbo, E. Canadell, P. Foury, and J. P. Pouget, *Science* **252**, 96 (1991).
- ¹⁰ S. Vallar and M. Goreaud, *J. Solid State Chem.* **129**, 303 (1997).
- ¹¹ W. H. Zachariasen, *J. Less-Common Met.* **62**, 1 (1978); I. D. Brown and K. K. Wu, *Acta Crystallogr., Sect. B: Struct. Crystallogr. Cryst. Chem.* **32**, 1957 (1976).
- ¹² H. Vincent and M. Marezio, in *Low-Dimensional Electronic Properties of Molybdenum Bronzes and Oxides*, edited by C. Schlenker (Kluwer, Dordrecht, 1989), p. 49.
- ¹³ P. Hohenberg and W. Kohn, *Phys. Rev.* **136**, 864 (1964).
- ¹⁴ W. Kohn and L. J. Sham, *Phys. Rev.* **140**, 1133 (1965).
- ¹⁵ P. Ordejón, E. Artacho, and J. M. Soler, *Phys. Rev. B* **53**, R10441 (1996).
- ¹⁶ P. Ordejón, E. Artacho, and J. M. Soler, in *MRS Symposia Proceedings No. 408* (Materials Research Society, Pittsburgh, 1996), p. 85.
- ¹⁷ D. Sánchez-Portal, P. Ordejón, E. Artacho, and J. M. Soler, *Int. J. Quantum Chem.* **65**, 453 (1997).
- ¹⁸ E. Artacho, D. Sánchez-Portal, P. Ordejón, A. García, and J. M. Soler, *Phys. Status Solidi B* **215**, 809 (1999).
- ¹⁹ P. Ordejón, *Phys. Status Solidi B* **217**, 335 (2000).
- ²⁰ J. P. Perdew, K. Burke, and M. Ernzerhof, *Phys. Rev. Lett.* **77**, 3865 (1996).
- ²¹ N. Troullier and J. L. Martins, *Phys. Rev. B* **43**, 1993 (1991).
- ²² L. Kleinman and D. M. Bylander, *Phys. Rev. Lett.* **48**, 1425 (1982).
- ²³ S. G. Louie, S. Froyen, and M. L. Cohen, *Phys. Rev. B* **26**, 1738 (1982).
- ²⁴ O. F. Sankey and D. J. Niklewski, *Phys. Rev. B* **40**, 3979 (1989).
- ²⁵ I. L. Garzón, K. Michaelian, M. R. Beltrán, A. Posada-Amarillas, P. Ordejón, E. Artacho, D. Sánchez-Portal, and J. M. Soler, *Phys. Rev. Lett.* **81**, 1600 (1998).
- ²⁶ D. Sánchez-Portal, J. Junquera, P. Ordejón, A. García, E. Artacho, and J. M. Soler, *Phys. Rev. Lett.* **83**, 3884 (1999).
- ²⁷ M. Calleja, C. Rey, M. M. G. Alemany, L. J. Gallego, P. Ordejón, D. Sánchez-Portal, E. Artacho, and J. M. Soler, *Phys. Rev. B* **60**, 2020 (1999).
- ²⁸ J. Izquierdo, A. Vega, L. C. Balbás, D. Sánchez-Portal, J. Junquera, E. Artacho, J. M. Soler, and P. Ordejón, *Phys. Rev. B* **61**, 13 639 (2000).
- ²⁹ J. Wang, J. Hallmark, D. S. Marshall, W. J. Ooms, P. Ordejón, J. Junquera, D. Sánchez-Portal, E. Artacho, and J. M. Soler, *Phys. Rev. B* **60**, 4968 (1999).
- ³⁰ J. I. Pascual, J. Gómez-Herrero, A. Baró, D. Sánchez-Portal, E. Artacho, P. Ordejón, and J. M. Soler, *Chem. Phys. Lett.* **321**, 78 (2000).
- ³¹ G. Fabricius, E. Artacho, D. Sánchez-Portal, P. Ordejón, D. A. Drabold, and J. M. Soler, *Phys. Rev. B* **60**, 16 283 (1999).
- ³² P. A. Fedders, D. A. Drabold, P. Ordejón, G. Fabricius, D. Sánchez-Portal, E. Artacho, and J. M. Soler, *Phys. Rev. B* **60**, 10 594 (1999).
- ³³ D. Sánchez-Portal, E. Artacho, J. M. Soler, A. Rubio, and P. Ordejón, *Phys. Rev. B* **59**, 12 678 (1999).
- ³⁴ M. S. C. Mazzoni, H. Chacham, P. Ordejón, D. Sánchez-Portal, J. M. Soler, and E. Artacho, *Phys. Rev. B* **60**, 2208 (1999).
- ³⁵ A. Rubio, D. Sánchez-Portal, E. Artacho, P. Ordejón, and J. M. Soler, *Phys. Rev. Lett.* **82**, 3520 (1999).
- ³⁶ E. Burgos, E. Halac, R. Weht, H. Bonadeo, E. Artacho, and P. Ordejón, *Phys. Rev. Lett.* **85**, 2328 (2000).
- ³⁷ D. Sánchez-Portal, I. Souza, and R. M. Martin, *Proceedings of the Workshop on "Fundamental Physics of Ferroelectrics"*, Aspen Center for Physics (in press).
- ³⁸ We have recently calculated the band structure of the blue bronze $K_{0.3}MoO_3$, obtaining an excellent agreement with the experimental results, P. Ordejón and E. Canadell (to be published).
- ³⁹ Note that the current implementations of DFT are known to underestimate the gap of semiconducting systems, so the real gap will be probably larger than the one obtained here.
- ⁴⁰ E. Canadell and M.-H. Whangbo, *Inorg. Chem.* **27**, 228 (1988).
- ⁴¹ E. Canadell, M. Evain, M. Ganne, and M.-H. Whangbo, *J. Solid State Chem.* **105**, 434 (1993).
- ⁴² M. Tournoux, M. Ganne, and Y. Piffard, *J. Solid State Chem.* **96**, 141 (1992).